An Improved Flux Observer Based on PLL Frequency Estimator for Sensorless Vector Control of Induction Motors

Mihai Comanescu, *Student Member, IEEE*, and Longya Xu, *Fellow, IEEE*

***Abstract*—This paper presents an improved method of flux estimation for sensorless vector control of induction motors based on a phase locked loop (PLL) programmable low-pass filter (LPF) and a vector rotator. A PLL synchronized with the voltage vector is used for stator frequency estimation. The pure integration of the stator voltage equations is difficult to implement and LPFs with a fixed cutoff provide good estimates only in the relatively high frequency range—at low frequencies, the estimates fail in both magnitude and phase. The method proposed corrects the above problem for a wide range of speeds. Simulations and experimental results on a 0.25-hp three-phase induction machine verify the validity of the approach.**

***Index Terms*—Induction machine, phase locked loop (PLL), sensorless control, vector control.**

NOMENCLATURE

$V_{\rm s} = [V_\alpha, V_\beta]$	Stator voltage in stationary reference frame.
$I_{\rm s} = [I_\alpha, I_\beta]$	Currents in stationary reference frame.
$e_{\rm s} = [e_\alpha, e_\beta]$	Back EMFs in stationary reference frame.
$\lambda_{\rm s} = [\lambda_{\alpha{\rm s}}, \lambda_{\beta{\rm s}}]$	Stator fluxes in stationary reference frame.
$\lambda_{\rm r} = [\lambda_{\alpha{\rm r}}, \lambda_{\beta{\rm r}}]$	Rotor fluxes in stationary reference frame.
V_d, V_q	Voltages in synchronous reference frame.
I_d, I_q	Currents in synchronous reference frame.
$V_{a{\rm n}}$, $V_{b{\rm n}}$	Line-neutral voltages.
$\omega_{\rm s}$	Synchronous frequency.
$\omega_{\rm r}$	Rotor mechanical speed.
$n_{\rm p}$	Number of pole pairs.
$R_{\rm s}$	Stator resistance.
$L_{\rm m}$	Magnetizing inductance.
$L_{\rm s}$, $L_{\rm r}$	Stator and rotor total inductances.
$T_{\rm r}$	Rotor time constant.
$\omega_{\rm c}$	LPF cutoff frequency.
$\lambda_{\rm s}^1$	Intermediate stator flux vector.
k	Ratio of cutoff frequency to stator frequency.
e_α^{dc}, e_β^{dc}	dc offsets of α, β back EMFs.
$\theta_{\rm v}$	Angle of stator voltage vector.
$\theta_{\rm r}$	Angle of rotor flux vector.
$T_a, T_b, T_{\rm c}$	Duty cycles of the inverter switches.
$\sigma = 1 - L_{\rm m}^2/L_{\rm s}L_{\rm r}$	Leakage factor.

Manuscript received April 21, 2004; revised September 10, 2004. Abstract published on the Internet November 25, 2005.

M. Comanescu was with the Department of Electrical and Computer Engineering, The Ohio State University, Columbus, OH 43210 USA. He is now with Azure Dynamics, Woburn, MA 01801-2103 USA.

L. Xu is with the Department of Electrical and Computer Engineering, The Ohio State University, Columbus, OH 43210 USA (e-mail: xu.12@osu.edu).

Digital Object Identifier 10.1109/TIE.2005.862317

I. INTRODUCTION

ESTIMATION of the fluxes using the voltage model (VM) observer is a convenient method for the sensorless vector control of induction motor drives. Techniques based on rotor equations require knowledge of the mechanical speed and depend heavily on the accuracy of the rotor time constant. Full order observers are more difficult to implement and rely on an even larger set of machine parameters [1]–[6].

The VM observer is both attractive and important for several reasons. First, if necessary, the critical parameter $(R_{\rm s})$ can be estimated in real time by using stator-mounted temperature sensors [7], and accurate stator fluxes can be obtained. Second, the coefficients in the equations linking the stator and rotor fluxes do not vary significantly with operating conditions [8]; thus, a good estimation of the rotor fluxes is possible and the decoupled rotor direct field orientation (DFO) method can be used. Third, dual-flux model reference adaptive system (MRAS) observers use the VM as a reference in order to estimate the motor speed. Finally, the estimate of the flux angle (in either stator or rotor DFO method) is crucial for the stability and the performance of a sensorless drive.

Many researchers have addressed issues related to flux observers and the main practical difficulty is well known—the offsets and drifts present in the motor back electromotive forces (EMFs) make the pure integration very difficult. To solve this problem, most methods described in the literature avoid the pure integration and are based on low-pass filters (LPFs) with either a fixed or a variable cutoff frequency [1]–[8]. An offset compensation method and a pure integration have been reported in [9], [10]. Excellent experimental results are reported at a low frequency; however, the complexity, computational burden, and accuracy issues almost prohibit its implementation on a low-cost fixed-point processor.

The synthesis of the stator fluxes using a fixed-cutoff LPF is easy to implement. Selection of an appropriate cutoff frequency can be done by experimental trials (usual values are 2–4 Hz); generally, this value depends on the hardware setup, quality of voltage, current feedback signals, A–D conversion precision, system noise, etc. With the above LPF replacing the

pure integrator, the dc offset problem can be largely alleviated and the flux estimates are close to the real ones if the stator frequency is five times or higher than the filter cutoff. However, the magnitude and angle errors are significant in the lower frequency range; this is briefly reviewed in Section II.

Three new integration algorithms are presented in [11], where fixed cutoff filters and feedback are used to emulate a pure integration. The method most suited for ac machine flux estimation exploits the orthogonality of the back EMF and stator flux vectors.

Programmable LPFs are used in [1]–[3] and [7] for the stator flux estimation. The $\alpha\beta$-axis back EMFs are fed into variable-cutoff filters, and the outputs are corrected by a vector rotator. Filter constants and vector-rotator parameters are functions of the stator frequency (which must be estimated). Therefore, the accuracy of the frequency estimate is a key factor in the overall flux-estimation method. In [1]–[3], the stator frequency is computed based on the induction-machine equations.

In this paper, this method is proposed—the stator fluxes are synthesized using programmable LPFs and a vector rotator similar to [1]–[3]. The novelty is that, for this type of application, the stator frequency is estimated with a phase locked loop (PLL). The PLL synthesizes a rotating reference frame that always tries to instantaneously align with the machine's voltage vector. The stator frequency is a stable by-product of the PLL process. The idea of using a PLL for frequency estimation comes from uninterruptible power supply (UPS) systems and was inspired by [12].

The PLL only uses the voltage vector and is likely to yield a better frequency estimate under real conditions (imperfections, offsets, etc.) than the method based on the machine's equations.

Simulations and experimental results show that, with proper tuning, the PLL can estimate the stator frequency with a sufficient bandwidth. Overall, good flux estimates are obtained and the method can be used for sensorless field orientation control of induction motors with improved performance.

II. VM Observer With Fixed-Cutoff LPF

The VM observer estimates the stator and rotor fluxes according to

$$\lambda_{\rm s} = \int (V_{\rm s} - R_{\rm s} I_{\rm s}) dt = \int e_{\rm s} dt \tag{1}$$

$$\lambda_{\rm r} = \frac{L_{\rm r}}{L_{\rm m}} (\lambda_{\rm s} - L_{\rm s} \sigma I_{\rm s}). \tag{2}$$

With the pure integrator replaced by an LPF with the cutoff frequency $\omega_{\rm c}$, the relationship between the stator flux and back EMF becomes

$$\frac{\lambda_{\rm s}}{e_{\rm s}} = \frac{1}{s + \omega_{\rm c}}. \tag{3}$$

The magnitude and phase errors between the flux vector obtained by (3) and the flux vector that would result from pure integration are

$$\varepsilon_{\rm mag} = \frac{\omega_{\rm s}}{\sqrt{\omega_{\rm s}^2 + \omega_{\rm c}^2}} \tag{4}$$

$$\varepsilon_{\rm phase} = \frac{\pi}{2} - \tan^{-1} \frac{\omega_{\rm s}}{\omega_{\rm c}}. \tag{5}$$

At low values of $\omega_{\rm s}$, the estimator yields a flux vector whose magnitude is smaller than real and whose phase lags to the back EMF by an angle less than 90°. As $\omega_{\rm s}$ increases, $\varepsilon_{\rm mag}$ tends to 1 while $\varepsilon_{\rm phase}$ tends to 0 and the estimate is close to the real flux. Additional details regarding the traditional VM observer and the errors occurring when integrators are substituted by LPFs can be found in [1]–[4].

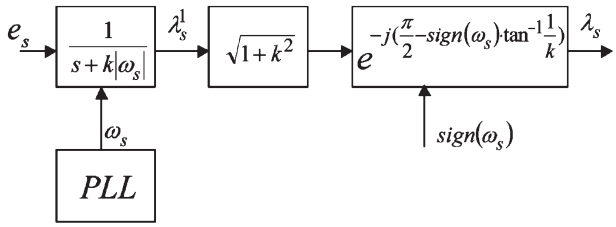

Fig. 1. Block diagram of the programmable LPF and the vector rotator.

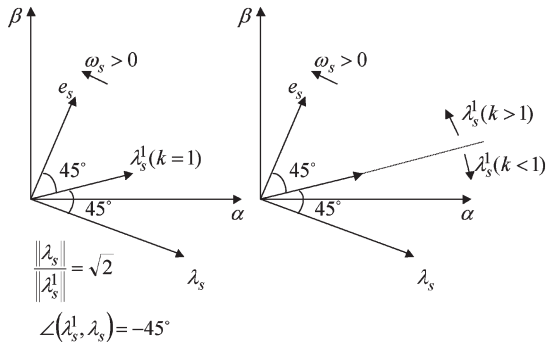

Fig. 2. Position of vector $\lambda_{\rm s}^1$ as a function of the design parameter k.

III. VM Observer With Programmable LPF

Fig. 1 shows the block diagram of the proposed programmable LPF and vector rotator.

The $\alpha\beta$ components of the back-EMF vector are fed into the two LPFs whose cutoff frequency is k times the estimated stator frequency. The output of the LPFs $(\lambda_{\rm s}^1)$ is compensated in magnitude and phase to obtain the flux vector that would result from an analytical integration of (1). The overall structure of the estimator is designed to emulate the frequency function of a pure integrator and to avoid output saturation. This is basically similar to the methods in [1]–[3]. Fig. 2 shows a vector diagram and the position of $\lambda_{\rm s}^1$ as a function of k. For $k = 1$, the intermediate vector $\lambda_{\rm s}^1$ lags the back EMF by 45° and its magnitude is $\sqrt{2}$ times smaller than that of the vector $\lambda_{\rm s}$. As k increases, $\lambda_{\rm s}^1$ lags the back EMF by an angle less than 45° and its magnitude decreases. In implementation, the

$\alpha\beta$ components of $\lambda_{\rm s}^1$ are available at every sampling time. For $\omega_{\rm s} > 0$, the pair of stator fluxes $\lambda_{\alpha{\rm s}}$, $\lambda_{\beta{\rm s}}$ is constructed as

$$\lambda_{\alpha{\rm s}} = \sqrt{1+k^2}\left(\lambda_{\alpha{\rm s}}^1 \cos\varphi + \lambda_{\beta{\rm s}}^1 \sin\varphi\right) \tag{6}$$

$$\lambda_{\beta{\rm s}} = \sqrt{1+k^2}\left(-\lambda_{\alpha{\rm s}}^1 \sin\varphi + \lambda_{\beta{\rm s}}^1 \cos\varphi\right) \tag{7}$$

$$\varphi = \frac{\pi}{2} - \tan^{-1}\left(\frac{1}{k}\right). \tag{8}$$

Since k is a constant, the compensation gain and the sine and cosine of the compensation angle can be computed off-line. The performance of this estimator depends mainly on the accuracy of the $\omega_{\rm s}$ estimate but also on the choice of k. Thus, at high values of k, the cutoff frequency of the LPF is high, and this helps attenuate the offsets present in the back EMFs. However, the compensation gain is also high and the vector rotator reamplifies the offsets. A steady-state offset analysis can be performed to estimate the worst case offsets that appear in the flux components $\lambda_{\alpha{\rm s}}$, $\lambda_{\beta{\rm s}}$. If the offsets at the LPF inputs are denoted as e_α^{dc} and e_β^{dc}, the maximum offsets at the compensator output are

$$\lambda_{\alpha,\max}^{dc} = \lambda_{\beta,\max}^{dc} = \frac{\sqrt{1+k^2}}{k} \cdot \frac{1}{|\omega_{\rm s}|}\left(\left|e_\alpha^{dc}\right| + \left|e_\beta^{dc}\right|\right). \tag{9}$$

The expression above shows that output offsets are frequency dependent and the behavior may worsen if $\omega_{\rm s}$ is very small. Comparison to the offsets yielded by a fixed-cutoff LPF, assuming $k = 1$ and $|e_\alpha^{dc}| = |e_\beta^{dc}|$, shows that the programmable LPF is better for frequencies $\omega_{\rm s} \geq 2\sqrt{2}\omega_{\rm c}$. An additional feature of the estimator is the existence of an optimal k; $k = 1$ minimizes the first factor in (9).

The biggest disadvantage of this method is the requirement of the vector rotator to know the sign of the stator frequency. For low and especially near zero frequency, $\omega_{\rm s}$ may temporarily change sign or oscillate around zero. The uncertainty in the sign of $\omega_{\rm s}$ seriously upsets the angle compensation.

IV. Description of the Phase Locked Loop

A typical three-phase UPS system uses two power feeders. Input voltages of the first feeder are rectified and feed the dc bus of an inverter. The second feeder (also called bypass) is used as backup and is supposed to take over the loads if any fault develops in the power conditioning circuit. This brings the problem of synchronizing the output voltages of the inverter with those of the bypass. Synchronization is required only if the frequency of the bypass is within acceptable limits (59–61 Hz). A PLL can be used to slowly lock the inverter output voltage vector to the bypass vector from any initial condition. The stability and dynamics of the synchronization are relatively easy to achieve because the bypass voltage has an almost constant magnitude and its frequency varies slowly in the 60-Hz vicinity.

Conditions are much tougher for a PLL intended for a frequency estimation in an induction machine (IM) drive. This is because the reference vector likely changes its frequency (and its magnitude) much faster during transients. Additionally, an estimation for a wider range and for both positive and negative frequencies must be achieved. The block diagram of the PLL proposed in this paper is shown in Fig. 3.

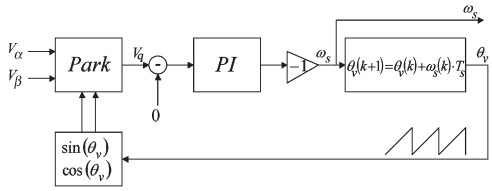

Fig. 3. Proposed PLL for frequency estimation in IM drives.

For the PLL shown above, the stator voltage is used as a reference vector. The PLL synthesizes the voltage angle $\theta_{\rm v}$; this is the angle of a rotational reference frame that is aligned with vector $V_{\rm s}$. At any sampling time, the correct angle is found if either (10) or (11) is true.

$$V_d = \|V_{\rm s}\| \tag{10}$$

$$V_q = 0. \tag{11}$$

The projection of the voltage vector on the q-axis of this reference frame is used as the error signal in order to enforce (11). The components V_α, V_β are transformed into the rotational reference frame given by $\theta_{\rm v}$ and $-V_q$ is fed into a proportional and integral (PI) controller. The PI output is the frequency estimate and is used in the integration of $\theta_{\rm v}$.

An important feature of this PLL is that the accuracy of frequency estimation depends only on the quality of the reference vector. In a sensorless controlled IM drive, the stator voltage is the very clean vector available (compared to current, flux, etc.), especially if stator voltages are constructed using the switching states of the inverter, noise, and offsets kept to a minimum. Additionally, the voltage vector has a considerable magnitude and produces a consistent large-enough error signal at the input of the PI block in Fig. 3.

In the previously published work [1]–[3], the synchronous frequency was determined based on IM (12) as

$$\omega_{\rm s} = \frac{(V_\beta - R_{\rm s} I_\beta)\lambda_\alpha - (V_\alpha - R_{\rm s} I_\alpha)\lambda_\beta}{\lambda_\alpha^2 + \lambda_\beta^2}. \tag{12}$$

The offsets and distortions in the fluxes and back EMFs, the dependence on stator resistance, and the decreasing magnitude of the numerator at low speeds deteriorate the $\omega_{\rm s}$ estimate.

V. Control System Description

The overall structure of the control system used in this paper is presented in Fig. 4. The system uses a rotor direct field orientation control. Both a fixed-cutoff LPF and a programmable LPF have been used for stator flux estimation and their outputs are compared.

The angle of the rotor flux is computed using

$$\theta_{\rm r} = \tan^{-1}\frac{\lambda_{\beta,{\rm r}}}{\lambda_{\alpha,{\rm r}}}. \tag{13}$$

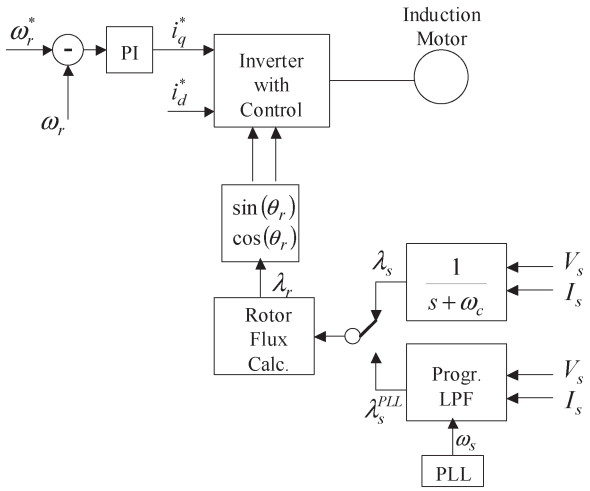

Fig. 4. Structure of the control system.

The rotor speed is estimated as

$$\omega_{\mathrm{r}} = \frac{1}{n_{\mathrm{p}}}\left(\omega_{\mathrm{s}} - \frac{L_{\mathrm{m}}}{T_{\mathrm{r}}} \cdot \frac{I_q}{|\lambda_{\mathrm{r}}|}\right). \tag{14}$$

The stator voltages (line-neutral) are obtained using the duty cycle of the inverter switches as

$$V_{a\mathrm{n}} = \frac{V_{dc}}{3}(2T_a - T_b - T_{\mathrm{c}}) \tag{15}$$

$$V_{b\mathrm{n}} = \frac{V_{dc}}{3}(-T_a + 2T_b - T_{\mathrm{c}}). \tag{16}$$

The stator voltages in the stationary reference frame are

$$V_\alpha = V_{a\mathrm{n}} \tag{17}$$

$$V_\beta = \frac{1}{\sqrt{3}}(V_{a\mathrm{n}} + 2V_{b\mathrm{n}}). \tag{18}$$

The system uses two stator flux estimators that run in parallel and one rotor flux calculator. To focus on evaluating the PLL-based flux estimation, there is no active flux control loop included.

VI. Simulation Results

The proposed control system has been simulated using Simulink. A sensorless IM drive simulation was set up. The motor is started using a traditional VM observer. The speed reference is set at 500 r/min and at $t = 0.3$ s, and the step changed to 1000 r/min. The load torque is 0.2 pu.

The dynamic performance of the PLL and the accuracy of the frequency estimation process are analyzed. The PLL is operated in parallel with the rest of the control system, and the stator frequency angle θ_{v} and voltage V_q are monitored.

Fig. 5 shows the real angle of the stator voltage vector and the estimated angle. In about 80 ms from startup, the angle estimated by the PLL has converged to the real angle. The speed reference change at $t = 0.3$ s produces very little disturbance in the angle estimation.

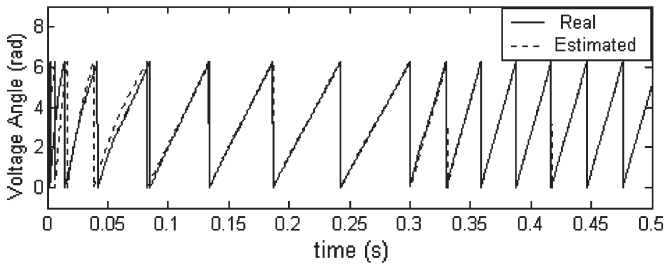

Fig. 5. Real and estimated voltage angle at startup.

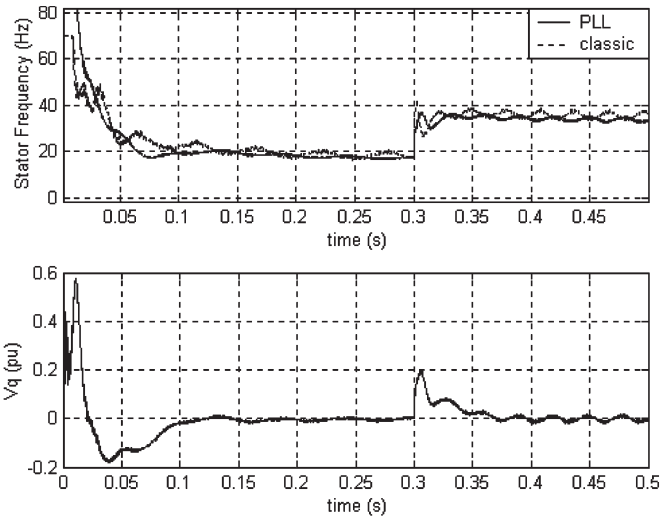

Fig. 6. Estimated frequency and V_q at startup.

Fig. 6 shows the frequency estimate by both the PLL and the classical method [using (12)]. The projection of the voltage vector on the q-axis of the PLL reference frame can also be seen.

In the simulation, the model adds noise and offsets (0.5% pu) to the measured voltages/currents in order to account for the signal acquisition hardware. In a real system, the projections of the voltage vector have superimposed ac components; this causes the estimation ripple in Fig. 6. At the end of the transient, the estimated frequency has stabilized, and the PLL holds V_q close to zero. When the step change at $t = 0.3$ s applies, the frequency estimate locks to the new value very quickly. On the other hand, it can be seen that the frequency estimated by the traditional method has more ripples than that by the PLL method (this is because the offsets in the current channels intervene). Also, implementation of (12) produces some steady-state error even in simulation; estimation only gets worse if the back EMFs or fluxes are distorted. The high-frequency burst at the start of the simulation comes from the aggressive tuning needed for the PI controller in Fig. 3.

Note that the final goal of using PLL is for the flux-estimation improvement. Fig. 7 compares the fluxes estimated by the PLL-based algorithm to the real motor fluxes.

As evidenced by the results, the estimated fluxes are very close to the real fluxes. The PLL-based programmable LPF successfully overcomes transient of the speed/frequency at 0.3 s and the estimated flux waveforms track the motor real fluxes

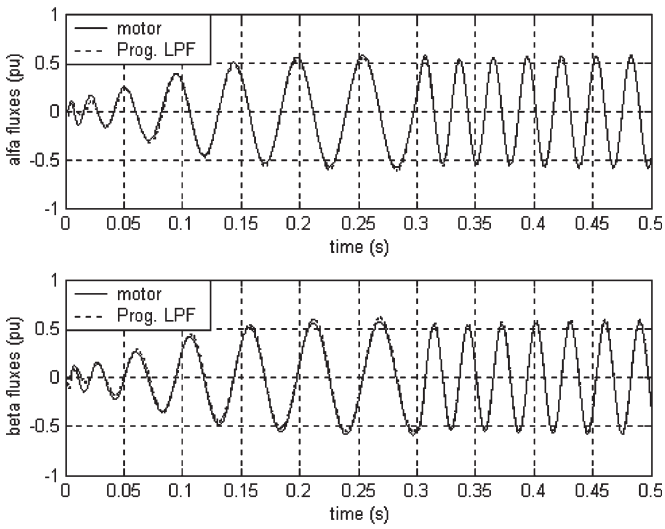

Fig. 7. Real and estimated rotor fluxes.

TABLE I
MOTOR SPECIFICATIONS AND PARAMETERS

Rating	*1/4 hp*	Pole #	4
Speed	*1732 rpm*	Voltage	220 V
R_s		10.9 Ω	
L_{ls}		0.015 H	
L_m		0.30 H	
Rr		5.57 Ω	

very well. It is also noticeable that for the initial several cycles, however, the flux estimates are not quite right. This can be attributed to the initial converging time needed by the PLL. It can be suspected that this estimator might not be able to provide flux information for the initial motor startup in the sensorless vector control mode.

VII. EXPERIMENTAL RESULTS

The induction motor used in the experimental testing is a typical three-phase squirrel cage machine. The specifications and parameters are listed in Table I.

The motor is powered by an insulated gate bipolar transistor (IGBT) inverter. The DSP for implementing the controller is a low cost, 16-bit fixed-point TMS320-F2407PGEA. The software of the controller is organized in two interrupts. A fast interrupt (50 μs) processes feedback signals, runs the classical VM observer and the PLL-based programmable LPF, computes the rotor flux angle and regulates the currents through two PI controllers. A slow interrupt (100 μs) estimates and regulates the rotor speed, executes the PLL algorithm and outputs the PWM commands. The inverter switching frequency is 10 kHz. The phase currents are measured through Hall sensors. Stator voltages are computed using (15)–(18) with a dc bus voltage sensor.

The initial investigation is focused on the dynamic performance of the PLL frequency estimator. To study that, a simple V/f algorithm was used to run the motor. A step change in frequency is applied and the dynamics of the PLL output is recorded. Fig. 8 shows the command and estimated frequency for a 9–27–9-Hz step changes.

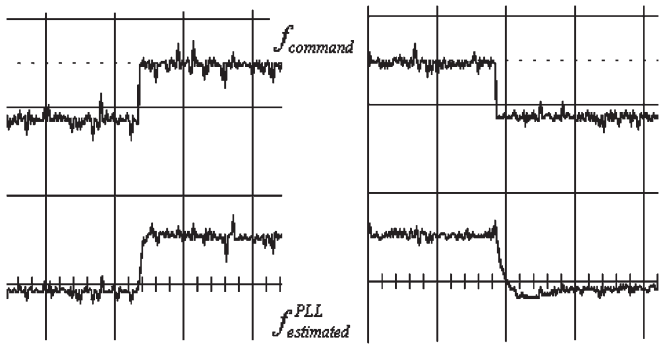

Fig. 8. Command and estimated frequency at 9–27–9-Hz step and 50 ms/div.

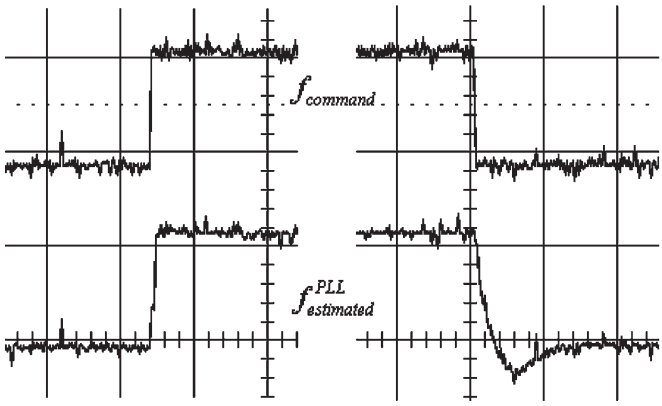

Fig. 9. Command and estimated frequency at 9–45–9-Hz step and 50 ms/div.

Fig. 9 shows the same waveforms for a 9–45–9-Hz change. Both tests are done at no load. It can be seen that, with proper tuning, the PLL can estimate the stator frequency with high bandwidth. The waveforms of $f_{\rm command}$ in both Figs. 8 and 9 should be noise-free step functions, however, all signals are shown noisy due to D/A and probe noise.

The second investigation is aimed at the stator flux waveforms produced by the PLL programmable LPF. The results are compared with those estimated by the classical observer. Both stator flux estimators run in parallel but only one rotor flux calculator is used due to DSP time constraints.

At a convenient stator frequency, the system is transitioned and field orientation is supported by the PLL-based programmable LPF. For comparison, the classical VM observer is implemented at the same time with a cutoff frequency of 19.98 rad/s (3.18 Hz); this was selected experimentally. Frequencies lower than 3.18 Hz were tried, but the obtained flux corresponding to (3) had significant offsets.

As discussed in the theory section, the PLL programmable LPF is expected to produce stator fluxes very close to those of the fixed-cutoff LPF for frequencies greater than $5\omega_{\rm c}$ (17 Hz). For lower frequencies, the classical observer's output is lagging the back EMFs by an angle less than 90° and leading the stator flux obtained by the programmable LPF.

Fig. 10 shows the α-axis signals obtained by the proposed method. The test is done at no load. The back EMF,

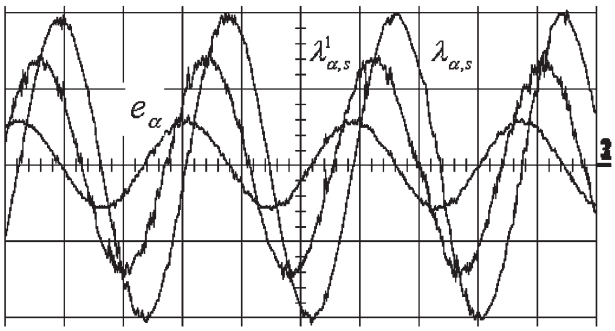

Fig. 10. Back EMF and stator flux by programmable LPF at $f = 18$ Hz, $k = 1$, and 20 ms/div.

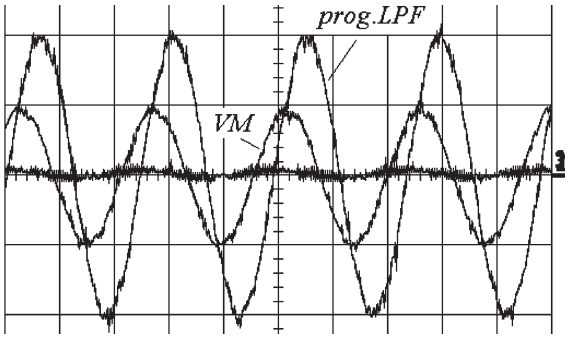

Fig. 11. Back EMF and stator fluxes by VM observer and PLL programmable LPF at $f = 2.1$ Hz and $k = 1$, 0.2 s/div.

intermediate flux $\lambda^1_{\alpha s}$, and the stator flux $\lambda_{\alpha s}$ are shown. The stator frequency is about 18 Hz, and $k = 1$. For $k = 1$, the stator flux $\lambda_{\alpha s}$ should lag $\lambda^1_{\alpha s}$ by 45° and its magnitude should be approximately $\sqrt{2}$ times bigger.

To verify the behavior of the PLL-based flux observer, Fig. 11 was obtained at a low frequency (approx. 2.1 Hz) where the difference between the two estimators is significant. The back EMF is very small and noisy. The output of the VM observer is incorrect in both magnitude and phase. The flux given by the PLL-based programmable LPF lags the back EMF by 90°.

Fig. 12 shows the stator flux estimate used as the input to the rotor-flux-calculator block at the moment of transition. The signal that commands the transition is on Channel (Ch.) 2. On the left side of Fig. 12, the field orientation control was done using the stator flux estimates produced by the classic VM observer. After transition, the fluxes produced by the PLL-based programmable LPF are used. The operating frequency for testing is approximately 8 Hz. Note the difference in magnitude and phase angle between the two stator flux estimators.

The behavior in terms of offsets can also be observed in Fig. 12. The fluxes given by the VM appear to have significant offsets and the waveforms are shifted—this is due to the analog channel and the A–D imbalance. Under the same circumstances, the programmable LPF yields flux waveforms that are more symmetric because of the higher cutoff frequency used.

Fig. 13 shows the flux waveforms for a 100–700 r/min step change in the speed command. The field orientation is supported with the PLL-based estimator. The test is done at no load. It can be seen that the flux maintains its correct angle and magnitude during the speed transient.

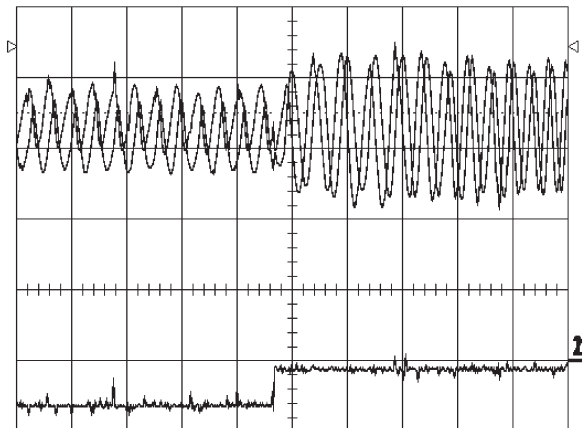

Fig. 12. Stator flux estimation from VM to PLL programmable LPF during transition at 200 ms/div.

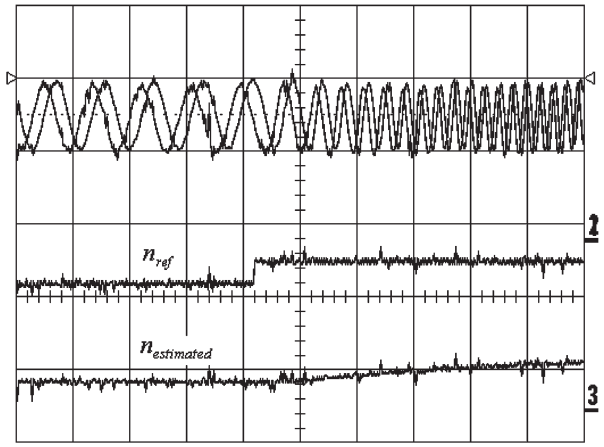

Fig. 13. Stator fluxes during 100–700 r/min step change at 100 ms/div.

VIII. Conclusion

This paper addresses the problems associated with the stator flux estimation in a sensorless vector control of induction motor drives. It is shown analytically and experimentally that the traditional VM observer produces significant estimation errors in the low-frequency range. If the stator frequency is known, a programmable LPF and a vector rotator can be used to correct the problem. Estimation of the stator frequency by a PLL is proposed and investigated. It is shown that a frequency estimation can be achieved with a high bandwidth and robustly in transient. Unlike the classical approach where frequency is estimated analytically, the PLL relies only on the stator voltage vector and is less influenced by offsets, distortions, or variations of the stator resistance. It is shown experimentally that stator fluxes obtained with the PLL-based estimator correct the magnitude and the phase errors of the traditional VM observer and improve the performance of sensorless vector control of IMs. The entire control algorithm is conveniently realized on a low-cost DSP chip.

REFERENCES

[1] M. H. Shin, D. S. Hyun, S. B. Cho, and S. Y. Choe, "An improved stator flux estimation for speed sensorless control of induction motors," in *Proc. IEEE Power Electronics Specialists Conf.*, Fukuoka, Japan, 1998, vol. 2, pp. 1581–1586.

[2] ——, "An improved stator flux estimation for speed sensorless stator flux orientation control of induction motors," *IEEE Trans. Power Electron.*, vol. 15, no. 2, pp. 312–317, Mar. 2000.

[3] M. Hinkkanen and J. Luomi, "Modified integrator for voltage model flux estimation of induction motors," in *Proc. IEEE 27th Annu. Conf. Industrial Electronics*, Denver, CO, 2001, vol. 2, pp. 1339–1343.

[4] N. R. N. Idris and A. H. M. Yatim, "An improved stator flux estimation in steady-state operation for direct torque control of induction machines," *IEEE Trans. Ind. Appl.*, vol. 38, no. 1, pp. 110–116, Jan./Feb. 2002.

[5] D. Hurst, T. G. Habetler, G. Griva, and F. Profumo, "Zero-speed tacholess IM torque control: Simply a matter of voltage integration," *IEEE Trans. Ind. Appl.*, vol. 34, no. 4, pp. 790–795, Jul./Aug. 1998.

[6] X. Xu and D. W. Novotny, "Implementation of direct stator flux orientation control on a versatile DSP based system," *IEEE Trans. Ind. Appl.*, vol. 27, no. 4, pp. 694–700, Jul./Aug. 1991.

[7] B. K. Bose, M. G. Simoes, D. R. Crecelius, K. Rajashekara, and R. Martin, "Speed sensorless hybrid vector controlled induction motor drive," in *Proc. 30th IAS Annu. Meeting*, Orlando, FL, Oct. 8–12, 1995, vol. 1, pp. 137–143.

[8] P. L. Jansen, R. D. Lorenz, and D. W. Novotny, "Observer-based direct field orientation: Analysis and comparison of alternative methods," *IEEE Trans. Ind. Appl.*, vol. 30, no. 4, pp. 945–953, Jul./Aug. 1994.

[9] J. Holtz, "Sensorless control of induction motor drives," *Proc. IEEE*, vol. 90, no. 8, pp. 1359–1383, Aug. 2002.

[10] J. Holtz and J. Quan, "Drift and parameter compensated flux estimator for persistent zero stator frequency operation of sensorless controlled induction motors," *IEEE Trans. Ind. Appl.*, vol. 39, no. 4, pp. 1052–1060, Jul./Aug. 2003.

[11] J. Hu and B. Wu, "New integration algorithms for estimating motor flux over a wide speed range," *IEEE Trans. Power Electron.*, vol. 13, no. 5, pp. 969–977, Sep. 1998.

[12] V. Kaura and V. Blasko, "Operation of a phase locked loop system under distorted utility conditions," *IEEE Trans. Ind. Appl.*, vol. 33, no. 1, pp. 58–63, Jan./Feb. 1997.

Mihai Comanescu (S'02) was born in Bucharest, Romania, in 1968. He received the B.S. degree from Bucharest Polytechnic Institute, Romania, in 1992 and the M.S. and Ph.D. degrees from The Ohio State University, Columbus, in 2001 and 2005, respectively, all in electrical engineering.

He is currently with Azure Dynamics, Woburn, MA, working on electric vehicle technology. His research interests include power electronics, ac drives, and motion control systems.

Longya Xu (S'89–M'90–SM'93–F'04) received the M.S. and Ph.D. degrees from the University of Wisconsin, Madison, in 1986 and 1990, respectively, all in electrical engineering.

He joined the Department of Electrical and Computer Engineering at The Ohio State University, Columbus, in 1990, where he is currently a Professor. He has served as a Consultant to many industry companies including Raytheon Company, U.S. Wind Power Company, General Motors, Ford, and Unique Mobility Inc. for various industrial concerns. His research and teaching interests include dynamic modeling and optimized design of electrical machines and power converters for variable speed generation and drive systems, application of advanced control theory, and digital signal processor for motion control and distributed power systems in super-high-speed operation.

Dr. Xu received the 1990 First Prize Paper Award from the Industrial Drives Committee, IEEE Industry Applications Society (IAS). In 1991, he won a Research Initiation Award from the National Science Foundation. He is also a recipient of the 1995 and 1999 Lumley Research Awards for his outstanding research accomplishments from the College of Engineering, The Ohio State University. He has served as the Chairman of the Electric Machine Committee of the IAS and an Associate Editor of IEEE TRANSACTIONS ON POWER ELECTRONICS.